

# Measurement of $dE_T/d\eta$ in Au+Au collisions at 200 GeV with sPHENIX at RHIC

Genki Nukazuka<sup>1,\*</sup>

<sup>1</sup>RIKEN Nishina Center for Accelerator-Based Science, Wako, Saitama 351-0198, Japan

**Abstract.** We report the first measurement of transverse energy ( $dE_T/d\eta$ ) in Au + Au collisions at 200 GeV using the sPHENIX detector at RHIC.  $dE_T/d\eta$  measurement provides key insights into quark-gluon plasma (QGP) formation and is one of the standard candles. The sPHENIX calorimeter system enables precise energy measurements, with detector response corrected using Monte Carlo simulations. Results show a strong centrality dependence, consistent with prior PHENIX and STAR data within uncertainties.

## 1 Introduction

sPHENIX, a state-of-the-art jet detector [1], was organized in 2011 at the Relativistic Heavy Ion Collider (RHIC) in Brookhaven National Laboratory (BNL) to complete the physics programs at RHIC. sPHENIX began operations in 2023 for the study of quark-gluon plasma (QGP) and cold-QCD. The sPHENIX detector is designed to have a large acceptance and high-rate capability and is optimized to measure jets and heavy quarks [2]. Jet-based observables like jet yield, jet substructure, and correlations of jets with other particles are great tools for the study of energy loss mechanism of partons with the QGP. The correlation between a high-energy photon and a jet is particularly useful as the photon does not interact with QGP directly while the jet does. Quark flavor dependence on energy loss with the QGP is an important key to understanding the nature of the QGP. The sPHENIX tracking system described in Sec. 2.2 can achieve a high resolution of DCA (distance of closest approach) to distinguish between prompt  $D_0$  and non-prompt  $D_0$ , which comes from the decay of  $B$  meson.

Transverse energy as a function of pseudorapidity ( $dE_T/d\eta$ ) is one of the standard candles in heavy-ion collisions. It can be used to estimate the Bjorken energy density [7], and previous measurements have indicated that the necessary condition for QGP formation is met in heavy-ion collisions at RHIC and LHC energies [3–6]. The sPHENIX calorimeter system is the key for the jet physics program, hence  $dE_T/d\eta$  measurement is a good starting point for sPHENIX.

## 2 The sPHENIX detector

The sPHENIX detector is the first in the RHIC experiments with a hadronic calorimeter at mid-rapidity, enabling reconstruction of the neutral component of jets. Measurements of gold+gold (Au + Au) collisions at the center-of-mass energy  $\sqrt{s_{NN}} = 200$  GeV explore

\*e-mail: [genki.nukazuka@riken.jp](mailto:genki.nukazuka@riken.jp)

a kinematic region different from that of the LHC experiments. This allows measurements in the low  $p_T$  region, which is challenging at LHC. The sPHENIX detector consists of a superconducting magnet, calorimetry system, tracking system, and forward detectors. The calorimetry and the tracking system cover pseudorapidity  $\eta$  from -1.1 to 1.1 for collisions within  $\pm 10$  cm from the center of the detector in the beam direction. The superconducting solenoid magnet, which was used at the BaBar experiment in SLAC, produces a magnetic field of 1.4 T in the beam direction.

## 2.1 Calorimeter system

The calorimeter system comprises an electromagnetic calorimeter (EMCal) and two layers of hadronic calorimeter (HCal), which are called the inner (IHCal) and outer (OHCal). The EMCal and IHCal are located inside the magnet, while the OHCal serves as the magnet flux return. The OHCal consists of steel absorber plates and plastic scintillators, and the IHCal consists of aluminum absorber plates and plastic scintillators.

The size of HCal towers is  $0.1 \times 0.1$  in  $\Delta\eta \times \Delta\phi$ . EMCal, which uses tungsten powder and scintillation fibers, was installed inside the inner HCal. EMCal is designed to be compact and has a fine segmentation of  $0.024 \times 0.024$  in  $\Delta\eta \times \Delta\phi$ .

## 2.2 Tracking system

The tracking detectors inside the calorimeters are the Time Projection Chamber (TPC), TPC Outer Tracker (TPOT), INTermediate silicon Tracker (INTT), and Monolithic active pixel sensor VerTeX detector (MVTX). Their roles are complemented: TPC gives a high momentum resolution, TPOT works for TPC calibration, INTT is for pile-up rejection and timing measurements, and MVTX allows precise vertex determination.

## 2.3 Forward detectors

There are three forward detectors: the Minimum Bias Detector (MBD), the sPHENIX event plane detector (sEPD), and the zero-degree calorimeter (ZDC). MBD provides minimum bias triggers and collision point reconstruction in the beam-axis by the measurements of the Cherenkov radiation of particles from collisions at both forward and backward positions. sEPD is a disc-shaped scintillation counter that provides excellent event plane resolution. ZDC is located far forward and works for centrality and luminosity measurements and issuing triggers.

# 3 Analysis

The detector construction was completed in March 2023, and the detector commissioning was conducted with Au + Au collision at the center-of-mass energy  $\sqrt{s_{NN}} = 200$  GeV in 2023. The data taken during the commissioning was used in the analysis.

The z-axis is defined along the direction of a beam towards the north, the y-axis points upward, and the x-axis completes the right-handed coordinate system.

## 3.1 Data selection

Data selection cuts were applied at the beginning of the analysis. First, the MBD trigger, which is firing at least two photomultiplier tubes on both north and south sides, was required.

Some selection criteria using the MBD and the ZDC were applied to remove beam-related backgrounds and non-hadronic collisions. Events with a collision point in the  $z$ -axis within  $\pm 20$  cm obtained by MBD were taken to avoid peripheral events in the tail of the distribution with large vertex resolution. Centrality percentiles were derived by fitting the MBD charge distribution through a convolution of particle production and event sampling based on a negative binomial distribution from Monte Carlo (MC) Glauber simulation [8–10]. Events with centrality from 0 to 60% are selected to ensure high event selection efficiency with a broad range of geometric configuration of the medium. The event selection achieved complete efficiency under the specified selection criteria.

### 3.2 The energy measurement and the correction

The electronic signals of each calorimeter tower are processed using a template fit obtained from the commissioning data and calibrated to the electromagnetic energy scale. The absolute energy scale calibrations for each pseudorapidity ring were performed with  $\pi^0 \rightarrow \gamma\gamma$  channel for EMCal and cosmic muons for HCal, respectively. The  $\eta$  region of EMCal from -1.1 to -0.9 was not included in this analysis since the EMCal readout electronics were only partially instrumented during this stage of commissioning.

The uncorrected  $dE_T/d\eta$  is calculated for a given centrality class as the sum of the transverse component of calorimeter tower energy  $E_T$  as a function of  $\eta$ , where  $E_T$  for each calorimeter tower is

$$E_{T,\text{tower}} = E_{\text{tower}} \sin \theta_T$$

Geant4-based MC simulation with three different event generators HIJING[11], AMPT[12], and EPOS[13] was performed to correct the reconstructed energy for the response of the calorimeters. The correction factor is defined as

$$C(\eta) = \frac{\sum_i E_{T,\text{tower}}(\eta, \phi_i)}{\sum_i E_{T,\text{particle}}(\eta, \phi_i)},$$

where the summations are taken over the full azimuthal angle  $\phi$ . The correction factors for each calorimeter sub-system are fairly constant with centrality. About 66% of MC truth  $dE_T/d\eta$  reconstructed by the EMCal, about 14% reconstructed by the OHCal, and about 4% by the IHCal in the calorimeter  $\eta$  acceptance with both the IHCal and OHCal calibrated to the EM scale. The ratio of reconstructed  $dE_T/d\eta$  to truth  $dE_T/d\eta$  for each calorimeter as a

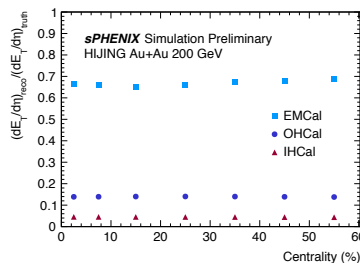


**Figure 1.** Mean correction factor value of reconstructed  $dE_T/d\eta$  for pseudorapidity from -0.5 to 0.5 divided by generator-level  $dE_T/d\eta$ , for sPHENIX calorimeter sub-systems as a function of centrality for range 0-60% centrality.

function of centrality can be found in figure 1. In this analysis, the EMCal and full HCal

(IHCal + OHCal) are used to make standalone measurements of the  $dE_T/d\eta$  and all three calorimeter layers (EMCal + IHCal + OHCal) are used for a full calorimeter measurement of  $dE_T/d\eta$ , where:

$$\frac{dE_T}{d\eta} = \frac{\sum E_{T,\text{tower}}(\eta)}{C(\eta)}.$$

### 3.3 $dE_T/d\eta$ distributions

Results for  $dE_T/d\eta$  as a function of  $\eta$  are presented in figure 2 for various centrality intervals. The  $dE_T/d\eta$  values for all three measurements with the sPHENIX EMCal, HCal, and full calorimeter have a strong dependence on centrality, increasing towards more central Au+Au collisions, whereas no significant dependence on  $\eta$  is seen. Additionally, these measurements are consistent with one another within uncertainties. The EMCal-only and HCal-only

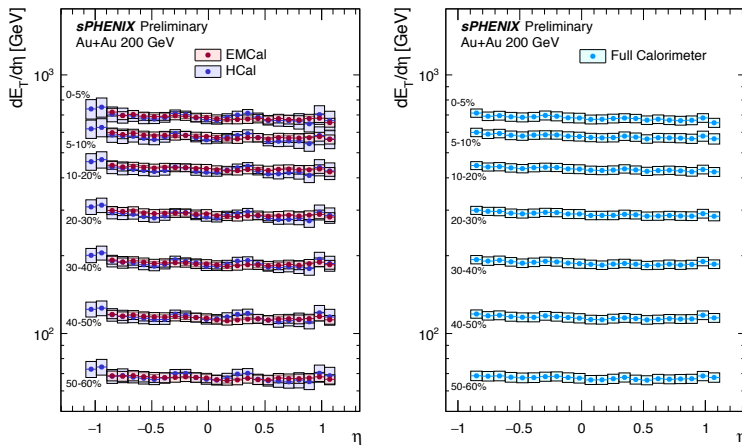
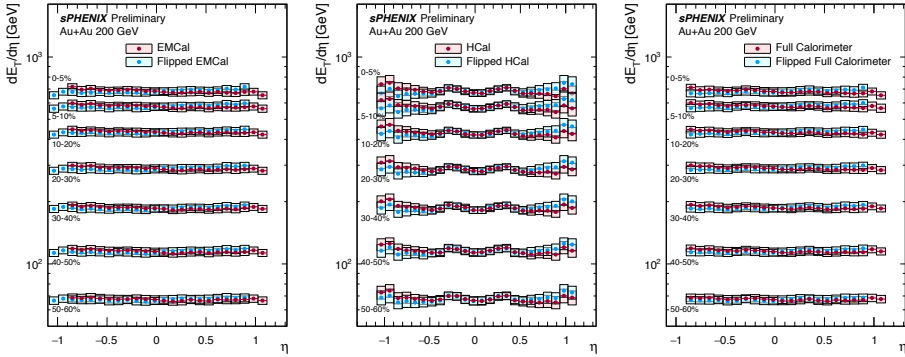


**Figure 2.** Fully corrected  $dE_T/d\eta$  measurements over the pseudorapidity range from -1.1 to 1.1 for HCal-only results and from -0.9 to 1.1 for EMCal-only and full calorimeter system results.

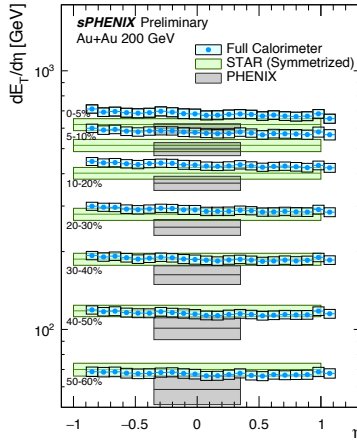
$dE_T/d\eta$  measurements are overlaid to highlight their agreement. This is a particularly encouraging result as the EMCal and HCal see different contributions of the collision energy. Further, for all calorimeter measurements,  $dE_T/d\eta$  at positive  $\eta$  and negative  $\eta$  are compatible within uncertainties.

Figure 3 is included here to highlight the symmetric nature of the EMCal-only, HCal-only and full calorimeter  $dE_T/d\eta$  results as a function of  $\eta$ . EMCal-only, HCal-only, and full calorimeter results are symmetric about  $\eta = 0$  within uncertainties.

Results from the sPHENIX full detector system for various centrality intervals are compared to the results from PHENIX [3] and STAR [4] in figure 4. The sPHENIX results are consistently higher than the results from PHENIX for all centrality bins but agree within uncertainties for mid-central bins 30-60%; the sPHENIX results are above the STAR results in the centrality range of 0-10% but are in agreement in other centrality intervals. Presently, these sPHENIX results use a preliminary centrality calculation for Run 2023 data which is likely to be updated for future reports of this analysis.



**Figure 3.** Comparison of fully corrected  $dE_T/d\eta$  measurements over the pseudorapidity range from -1.1 to 1.1 for HCal-only results and from -0.9 to 1.1 for EMCal-only and full calorimeter system results.



**Figure 4.** Fully corrected  $dE_T/d\eta$  measurements over pseudorapidity range from -0.9 to 1.1 using the full sPHENIX calorimeter system. STAR and PHENIX measurements are included for comparison.

## References

- [1] Reaching for the Horizon: The 2015 Long Range Plan for Nuclear Science. (2015). <https://www.osti.gov/biblio/1296778>
- [2] sPHENIX Collaboration, sPHENIX Technical Design Report (2019). <https://indico.bnl.gov/event/7081/>
- [3] A. Adare *et al.* (PHENIX Collaboration), Transverse energy production and charged-particle multiplicity at midrapidity in various systems from  $\sqrt{s_{NN}} = 7.7$  to 200 GeV. Phys. Rev. C **93**, 024901 (2016). <https://doi.org/10.1103/PhysRevC.93.024901>
- [4] J. Adams *et al.* (STAR Collaboration), Measurements of transverse energy distributions in Au + Au collisions at  $\sqrt{s_{NN}} = 200$  GeV. Phys. Rev. C **70**, 054907 (2004). <https://doi.org/10.1103/PhysRevC.70.054907>

- [5] J. Adams *et al.* (ALICE Collaboration), Measurement of transverse energy at midrapidity in Pb-Pb collisions at  $\sqrt{s_{\text{NN}}} = 2.76$  TeV. *Phys. Rev. C* **94**, 034903 (2016). <https://doi.org/10.1103/physrevc.94>.
- [6] S. Chatrchyan *et al.* (CMS Collaboration), Measurement of the Pseudorapidity and Centrality Dependence of the Transverse Energy Density in Pb-Pb Collisions at  $\sqrt{s_{\text{NN}}} = 2.76$  TeV. *Phys. Rev. Lett.* **109**, 152303 (2012). <https://doi.org/10.1103/PhysRevLett.109.152303>
- [7] J. D. Bjorken, Highly relativistic nucleus-nucleus collisions: The central rapidity region, *Phys. Rev. D* **27**, 140 (1983). <https://doi.org/10.1103/PhysRevD.27.140>
- [8] C. Loizides, J. Nagle, and P. Steinberg, Improved version of the PHOBOS Glauber Monte Carlo, *SoftwareX* **1-2**, 13 (2015). <https://doi.org/10.1016/j.softx.2015.05.001>
- [9] S. S. Adler *et al.* (PHENIX Collaboration), Systematic studies of the centrality and  $\sqrt{s_{\text{NN}}}$  dependence of the  $dE_T/d\eta$  and  $dN_{\text{ch}}/d\eta$  in heavy ion collisions at midrapidity. *Phys. Rev. C* **71**, 034908 (2005). <https://doi.org/10.1103/PhysRevC.71.034908>
- [10] A. Adare *et al.* (PHENIX Collaboration), Centrality categorization for Rp(d)+A in high-energy collisions. *Phys. Rev. C* **90**, 034902 (2014). <https://doi.org/10.1103/PhysRevC.90.034902>
- [11] X. Wang and M. Gyulassy, HIJING: A Monte Carlo model for multiple jet production in pp, pA, and AA collisions. *Phys. Rev. D* **44**, 3501 (1991). <https://doi.org/10.1103/PhysRevD.44>
- [12] Z. Lin, C. Ko, B. Li, B. Zhang, and S. Pal, Multiphase transport model for relativistic heavy ion collisions. *Phys. Rev. C* **72**, 064901 (2005). <https://doi.org/10.1103/physrevc.72.064901>
- [13] T. Pierog, Iu. Karpenko, J. M. Katzy, E. Yatsenko, and K. Werner, EPOS LHC: Test of collective hadronization with data measured at the CERN Large Hadron Collider. *Phys. Rev. C* **92**, 034906 (2015). <https://doi.org/10.1103/physrevc.92.034906>